

A numerical study for boundary layer current and sheet flow transport induced by a skewed asymmetric wave

CHEN Xin^{1*}, ZHANG Zichao², WANG Fujun¹

¹ Beijing Engineering Research Center of Safety and Energy Saving Technology for Water Supply Network System, China Agricultural University, Beijing 100083, China

² School of Electric Power, North China University of Water Resources and Electric Power, Zhengzhou 450045, China

Received 12 November 2017; accepted 26 February 2018

© Chinese Society for Oceanography and Springer-Verlag GmbH Germany, part of Springer Nature 2018

Abstract

An analytical model with essential parameters given by a two-phase numerical model is utilized to study the net boundary layer current and sediment transport under skewed asymmetric oscillatory sheet flows. The analytical model is the first instantaneous type model that can consider phase-lag and asymmetric boundary layer development. The two-phase model supplies the essential phase-lead, instantaneous erosion depth and boundary layer development for the analytical model to enhance the understanding of velocity skewness and acceleration skewness in sediment flux and transport rate. The sediment transport difference between onshore and offshore stages caused by velocity skewness or acceleration skewness is shown to illustrate the determination of net sediment transport by the analytical model. In previous studies about sediment transport in skewed asymmetric sheet flows, the generation of net sediment transport is mainly concluded to the phase-lag effect. However, the phase-lag effect is shown important but not enough for the net sediment transport, while the skewed asymmetric boundary layer development generated net boundary layer current and mobile bed effect are key important in the transport process.

Key words: analytical model, boundary layer current, sediment transport, sheet flow, skewed asymmetric wave

Citation: Chen Xin, Zhang Zichao, Wang Fujun. 2018. A numerical study for boundary layer current and sheet flow transport induced by a skewed asymmetric wave. *Acta Oceanologica Sinica*, 37(9): 82–89, doi: 10.1007/s13131-018-1267-4

1 Introduction

Oscillatory flows induced by short waves in nearshore zones are velocity-skewed with peaked narrow crest and flat wide trough in wave shoaling, and acceleration-skewed with steep frontal slope and gentle rear slope in a surf zone. In a sheet flow, a shear stress is large and a sediment concentration is high. The sediment transport is very essential under the velocity-skewed and acceleration-skewed (skewed asymmetric) oscillatory sheet flows because it is very important in the topography evolution. Knowledge of sediment transport in skewed asymmetric oscillatory sheet flows is required in coastal engineering which is related to velocity skewness and acceleration skewness.

The studies of the sediment transport under skewed asymmetric oscillatory sheet flows include purely velocity-skewed flows, purely acceleration-skewed flows and mixed flows with the velocity skewness and the acceleration skewness (Ruessink et al., 2009; Dong et al., 2013). Asymmetric development of a boundary layer thickness (Yuan and Madsen, 2015) and a large net sediment transport rate are observed with high velocity skewness (O'Donoghue and Wright, 2004b) or acceleration skewness (Watanabe and Sato, 2004). The generation of the net sediment transport is mainly attributed to the phase-lag both in velocity-skewed flows (Li et al., 2008) or acceleration-skewed flows (van der A et al., 2010). There are three types of phase-lag (Chen et al., 2018a): (1) a phase-shift which denotes the responded time of sediment movement in the sheet flow layer falling behind free stream velocity; (2) a phase-residual which denotes sediment en-

trained during the current half period, maintained in movement during deceleration stage, and transported after flow reversal; and (3) a phase-lead which denotes the leading time of bottom shear stress and boundary layer velocity to the free stream velocity. The above conclusions about the generation of net sediment transport (Li et al., 2008; van der A et al., 2010) and importance of each part of phase-lag are still not clear.

In the recent couple of decades, advanced empirical models considering phase-lag effects are established for sediment transport under skewed asymmetric oscillatory sheet flows. Most of the empirical models are half-periodic types following Dibajnia (1991) which only discontinuously consider the phase-residual above a critical value. To cover new measured data, more parameters related to the phase-residual are given (Dong et al., 2013), together with the acceleration and the asymmetric development of boundary layer thickness between onshore and offshore flow stages. Some empirical models are not easy to implement in engineering due to difficulties in calibrating abundant parameters. Some key factors are not considered, such as the impacts of the net current caused by the velocity skewness or acceleration skewness. Furthermore, half-periodic empirical models are lack in instantaneous sediment transport. To bridge the gap, advanced instantaneous models considering the phase-shift have been developed in the last decade (Gonzalez-Rodriguez and Madsen, 2007). However, the phase-lead and continuous appearance of the phase-residual are never seen in any instantaneous model, and the asymmetric boundary layer thickness is not either. None

Foundation item: The National Natural Science Foundation of China under contract Nos 51609244 and 51779258.

*Corresponding author, E-mail: chenx@cau.edu.cn

of the instantaneous models can be applied widely for sediment transport in velocity- and acceleration-skewed oscillatory sheet flows, and a proper exponent of a velocity power function for the instantaneous sediment transport rate should be selected accordingly (Chen et al., 2018b, c).

The sediment transport in the oscillatory sheet flow is a typical hyper-concentrated two-phase flow with a sediment volumetric concentration of about 0.08–0.60. To enhance the theory and relevant mechanism about the velocity skewness and the acceleration skewness, advanced two-phase numerical models are developed for skewed asymmetric oscillatory sheet flows in the recent two decades. A two-phase model is enabled to study instantaneous sediment transport and net sediment flux, and also erosion depth, phase-lag and boundary layer development. However, all variables in the two-phase model, such as phase-lag and boundary layer development, are hard to be separated for the actual effect of the velocity skewness or acceleration skewness in sediment transport. A basic problem is that the causes of the net sediment flux are still insufficiency known.

This study utilizes an instantaneous analytical model (Chen et al., 2018b, c) with the parameters settings from the two-phase model (Lee et al., 2016) for sediment transport in skewed asymmetric oscillatory sheet flows. Three types of the phase-lag and the boundary layer thickness are discussed. We will focus on the selection of exponents in the power function between the sediment transport rate and the velocity and skewed asymmetric characteristic. To isolate the effects of the velocity skewness and the acceleration skewness, we will examine (1) the purely velocity-skewed flows, and (2) the purely acceleration-skewed flows separately.

2 Methods and data

The analytical model (Chen et al., 2018b, c) consists of velocity and concentration profiles and the sediment transport rate. The two-phase model (Lee et al., 2016) supplies essential parameters for the analytical model.

2.1 Model and data description

Following Abreu et al. (2010), the free stream velocity (U) of skewed asymmetric oscillatory flow is imaginary part of

$$V + U_i = F \sum_{k=0}^{\infty} r^{-k} \times \exp\{i[(k+1)\sigma(t-t_0) + k\chi]\}, \quad (1)$$

where F is the free stream velocity amplitude; i is the imaginary unit; r and χ are wave form parameters; t is the time; $\sigma = 2\pi/T$, is the angular frequency; T is the period; and $t_0 = \sigma^{-1} \arcsin(r^{-1} \sin\chi)$, forces the free stream velocity being 0 at the time 0. Figure 1 shows a typical process of the free stream velocity, where $r > 1$ and $-\pi/2 < \chi < 0$; subscripts a and d denote acceleration and deceleration stages, respectively; subscripts c and t are the crest and trough stages, respectively; positive and negative symbols denote onshore and offshore directions, respectively.

The exponential approach of the velocity in the boundary layer is given by the following Nielsen and Guard (2010), that is,

$$V_b + U_{bi} = (V + U_i) \left\{ 1 - \exp \left[-(1 + \lambda i) \frac{y + Z}{\delta} \right] \right\}, \quad (2)$$

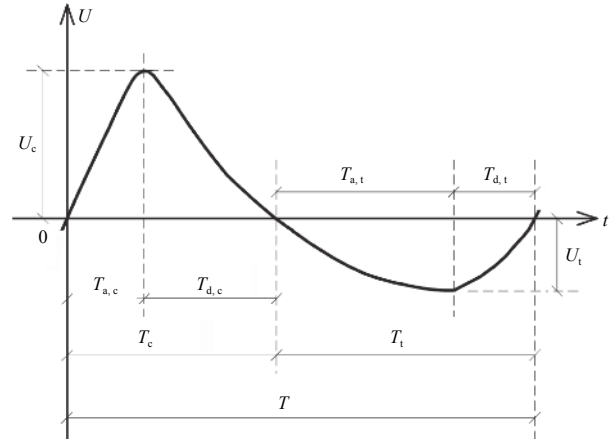


Fig. 1. Free stream velocity.

$$U_b = F \sum_{k=0}^{\infty} r^{-k} \{ \sin[(k+1)\sigma(t-t_0) + k\chi] - \exp \left(-\frac{y+Z}{\delta} \right) \times \sin \left[(k+1)\sigma(t-t_0) + k\chi - \lambda \frac{y+Z}{\delta} \right] \}, \quad (3)$$

where λ is the phase-lead parameter on the immobile bed surface; subscript b denotes the boundary layer; y is the vertical coordinate originally located at the initial undisturbed bed; Z is the erosion depth; $\delta = \delta_b/4.6$; and δ_b is the turbulent boundary layer thickness.

Chen et al. (2018b, c) applied an ideally exponential approach (Chen et al., 2013) to the real sediment volumetric concentration (C), which is

$$C = C_{\max} \exp \left[-(1 + \frac{y}{Z}) \right], \quad (4)$$

where subscript max denotes the maximum and $C_{\max} = 0.6$. Equation (4) considered the mass conservation, i.e., the integration of Eq. (4) above $y = -Z$ equal ZC_{\max} .

The integration of Eqs. (2) and (4) is

$$\int_{-Z}^{\infty} (V + U_i) \left\{ 1 - \exp \left[-(1 + \lambda i) \frac{y + Z}{\delta} \right] \right\} \times C_{\max} \exp \left[-(1 + \frac{y}{Z}) \right] dy = \frac{C_{\max} Z (V + U_i) (1 + \lambda i)}{(1 + \lambda i) + \delta/Z}. \quad (5)$$

The instantaneous transport rate is taken from the imaginary part of Eq. (5), that is,

$$q = C_{\max} Z \left[\frac{U(1 + \lambda^2 + \delta/Z) + V\lambda\delta/Z}{\lambda^2 + (1 + \delta/Z)^2} \right]. \quad (6)$$

Equation (6) consists of the free stream velocity, the bottom velocity phase-lead, the boundary layer thickness and the erosion depth. The instantaneous q is usually approximated by $q/q_{\max} = \text{sgn}(U)|U/U_{\max}|^n$, in which n is summarized in Chen et al. (2018b, c) which increases with the decrement of the phase-re-

sidual. Equation (6) is invalid for a progressive wave or wave-current flow, because Eq. (2) is only the analytical approach of the oscillatory flow (Chen et al., 2018c).

The model is available for analyzing the phase-lag and boundary layer development effect related to the velocity skewness and the acceleration skewness. λ , δ_b and Z are so far unknown and need calibration to determine. In the present study, an Eulerian two-phase model (Lee et al., 2016) is applied to determine λ , δ_b and Z . Here λ and δ_b are obtained by Eq. (3) using a least square method, with U_b and Z predicted by the two-phase model (Lee et al., 2016) that incorporates the rheological characteristic of sediment, and considers the enduring-contact, inertial, and fluid viscosity effects in a sediment pressure and stress for a wide range of particle Reynolds number. A k - ε turbulence model is adopted to compute the fluid Reynolds stresses, and a novel numerical scheme is proposed to avoid numerical instability caused by a high sediment concentration and allow the computation within and outside the sediment bed in Lee et al. (2016). Net q validation is shown in Fig. 2 for collected data in the oscillatory sheet flows which include purely velocity-skewed flows ($\chi = -\pi/2$) and purely acceleration-skewed flows ($\chi = 0$) (Dibajnia, 1991; Ribberink and Al-Salem, 1995; O'Donoghue and Wright, 2004b; Watanabe and Sato, 2004; Li et al., 2008; van der A et al., 2010; Dong et al., 2013). Good agreement between computation and experiment is obtained (Fig. 2).

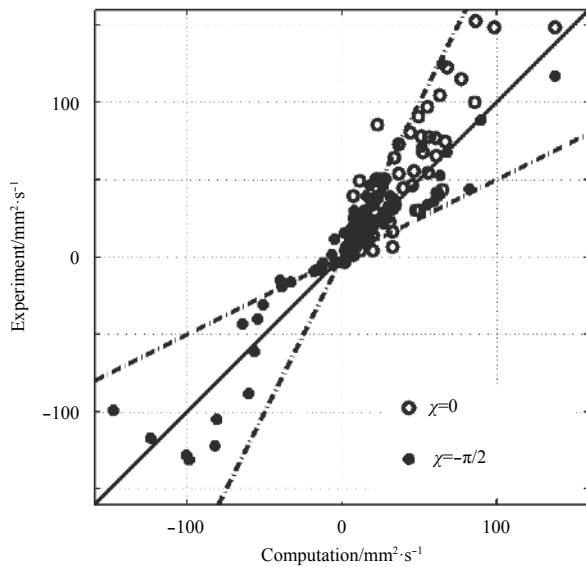


Fig. 2. Net q validation.

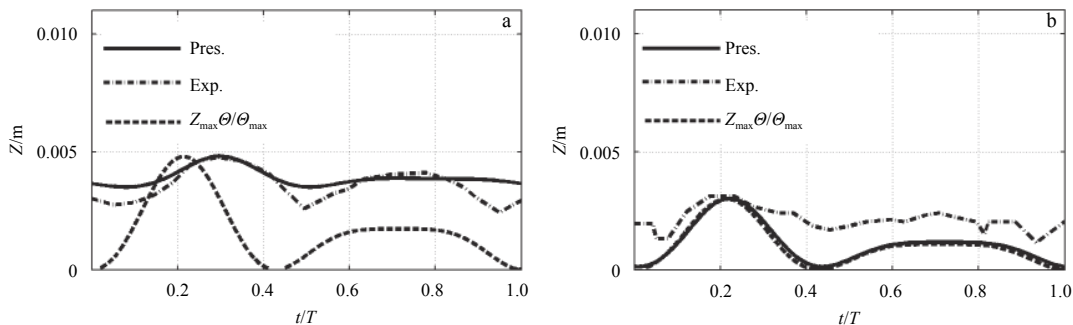


Fig. 3. Instantaneous Z in purely velocity-skewed flow ($T=7.5$ s, $U_t=0.9$ m/s and $U_{\max}=U_c=1.5$ m/s. θ is the Shields parameter). a. $D=0.13$ mm and b. $D=0.46$ mm.

2.2 Skewed asymmetric characteristic

In the velocity-skewed flow, the net sediment transport caused by a high velocity skewness is usually classified by the phase-lag. Sediment would be entrained very high by large U_{\max} that they cannot completely settle down with small D during short T before flow reversal. Offshore net q is observed when the phase-residual is very obvious with large U_{\max} , small D or short T . Onshore net q is observed when the phase-lag effect is small. On the basis of different phase-lag effects, Ribberink and Al-Salem (1995) explained the relation between net q and the velocity skewness, later Hassan and Ribberink (2010) added the influence of D and U_{\max} .

In the acceleration-skewed flow, the onshore net q is attributed to the phase-lag related to the acceleration skewness (van der A et al., 2010) denoted by $\beta = a_{\max}/(a_{\max} - a_{\min})$, where a is the acceleration. This means from $U = -U_t$ to $U = U_c$ (Fig. 1), small $T_{d,t}$ corresponding to large acceleration makes much sediment entrained in T_t remain in movement after flow reversal to be carried away during T_c . The process is opposite from $U = U_c$ to $U = -U_t$, so onshore net q is generated by different sediment amount between T_c and T_t . The onshore net q is enhanced when U_{\max} and β increase or D decreases, which lead to increments in the phase-lag related to the acceleration skewness.

The three parts of the phase-lag and the boundary layer thickness can be seen in Eq. (6), where the phase-shift and the phase-residual are included in the erosion depth Z (O'Donoghue and Wright, 2004a). So the previous conclusions (Ribberink and Al-Salem, 1995; Hassan and Ribberink, 2010; van der A et al., 2010) about the phase-lag related to the velocity skewness and the acceleration skewness can be contained. Furthermore, the effect of the boundary layer thickness (δ_b) also can be shown by δ in Eq. (6), where a larger δ_b corresponds to a smaller transport rate for the same Z .

3 Results and discussion

Generally, the following analysis is based on O'Donoghue and Wright (2004b) and van der A et al. (2010) cases in Table 1.

3.1 Purely velocity-skewed flows

To illustrate the phase-shift and the phase-residual, Fig. 3

Table 1. Cases for sediment transport study

Reference	Flow type	$U_{\max}/\text{m}\cdot\text{s}^{-1}$	D/mm	T/s
O'Donoghue and Wright (2004b)	$\chi = -\pi/2$	1.5	0.13, 0.46	7.5
van der A et al. (2010)	$\chi = 0$	1.3	0.15, 0.46	6.0

shows Z with $T=7.5$ s, $U_t=0.9$ m/s and $U_{max}=U_c=1.5$ m/s, where “Exp.” and “Pres.” denote the experiment and the present computation respectively. The velocity skewness parameter is $R=U_c/(U_c+U_t)=0.625$. The phase-lag parameter Ψ being $\sigma\Delta/w$ is the time ratio between the sediment falling down and the wave period introduced by [Dohmen-Janssen \(1999\)](#), where Δ is the sheet flow layer thickness and w is the sediment falling velocity. Ψ is 0.71 for $D=0.13$ mm case and is 0.10 for $D=0.46$ mm case. Accordingly, the phase-shift in [Fig. 3a](#) is about $0.08t/T$, and larger than $0.02t/T$ in [Fig. 3b](#), as the minimum Z moment falling behind $t/T=0$. The phase-residual for $D=0.13$ mm is also larger than that of $D=0.46$ mm: Z at T_t ($t/T=0.71$) is close to that at T_c ($t/T=0.21$) in [Fig. 3a](#) due to large phase-residual, while Z at T_t is obviously smaller than that at T_c in [Fig. 3b](#). If the phase-residual reduces to 0, minimum Z at flow reversal ($t/T=0.0$ or 0.42) is 0, and $Z/Z_{max}=\theta/\theta_{max}$. In $D=0.13$ mm case, $Z/Z_{max}=\theta/\theta_{max}$ cannot be used due to large phase-residual.

To explain the effect of boundary layer development, [Fig. 4](#) shows the instantaneous δ_b . The boundary layer developments of T_c ($t/T=0.0-0.42$) and T_t ($t/T=0.42-1.0$) stages are asymmetric in the velocity-skewed flow. The shear stress and roughness near the flow crest ($t/T=0.15-0.25$) are much larger than that near the flow trough ($t/T=0.6-0.8$) due to $U_c \gg U_t$, and δ_b (proportional to roughness) near the flow crest is larger than that near the flow trough.

The asymmetric development of δ_b caused by the velocity skewness leads to a net current in Eq. (3) at every y ([Fig. 5](#)). In [Fig. 4a](#), δ_b in T_c is almost larger than that in T_t , so the U_b/U near

flow crest is smaller than that near the flow trough in Eq. (3) based on $y+Z$, leading to offshore net U_b ([Fig. 5](#)). The offshore net U_b is observed ([O’Donoghue and Wright, 2004a, b](#)) and predicted by Eq. (3), which is also obtained based on y ([Fig. 5](#)) except onshore value in the sheet flow layer bottom for the mobile bed effect. Notice the velocity skewness parameter $R>0.5$, the lowest level mobilized by the strong U_c is immobile during T_t with a weak U_t , which is seen as the Z in [Fig. 3](#). With the increment of D (0.13–0.46 mm), the phase-residual decreases and the Z difference between onshore flow crest and offshore flow trough increases, so the onshore net U_b based on y increases from [Fig. 5a](#) to [Fig. 5b](#).

The net U_b causes net sediment flux $\phi_c = \langle U_b \rangle \langle C \rangle$, where the angle brackets denote the periodic average. The present computed ϕ_c , the wave related $\phi_w = \langle U_b' C' \rangle$ and the total flux $\phi = \phi_c + \phi_w$ are shown in [Fig. 5](#). The experimental (circle) net ϕ of $D=0.13$ mm ([Fig. 5a](#)) near the bed is clearly offshore, while the ϕ of $D=0.46$ mm ([Fig. 5b](#)) is generally onshore. The offshore ϕ of $D=0.13$ mm is concluded to large phase-lag in previous study, where obvious phase-lag makes a large amount of sediment entrained in T_c remain in suspension after flow reversal to be carried away at T_t contributing offshore ϕ . The onshore ϕ of $D=0.46$ mm is concluded to small phase-lag, where Z is proportional to U^2 and ϕ is proportional to ZU , thus the net ϕ is proportional to the velocity skewness $\langle U^3 \rangle$. The data for the $D=0.46$ mm are scattered due to C measurement uncertainty. However, the present prediction almost passes the centre of the data, and has the same shape as that fitted by [O’Donoghue and Wright \(2004b\)](#). Over all, the

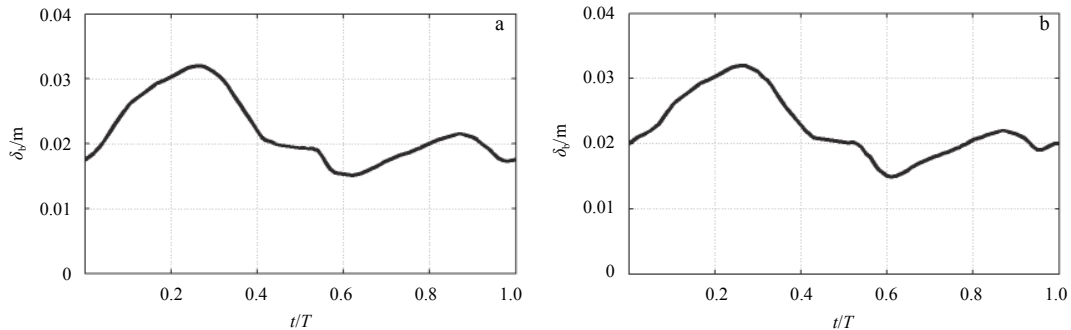


Fig. 4. Boundary layer thickness development in purely velocity-skewed flow ($T=7.5$ s, $U_t=0.9$ m/s and $U_{max}=U_c=1.5$ m/s). a. $D=0.13$ mm and b. $D=0.46$ mm.

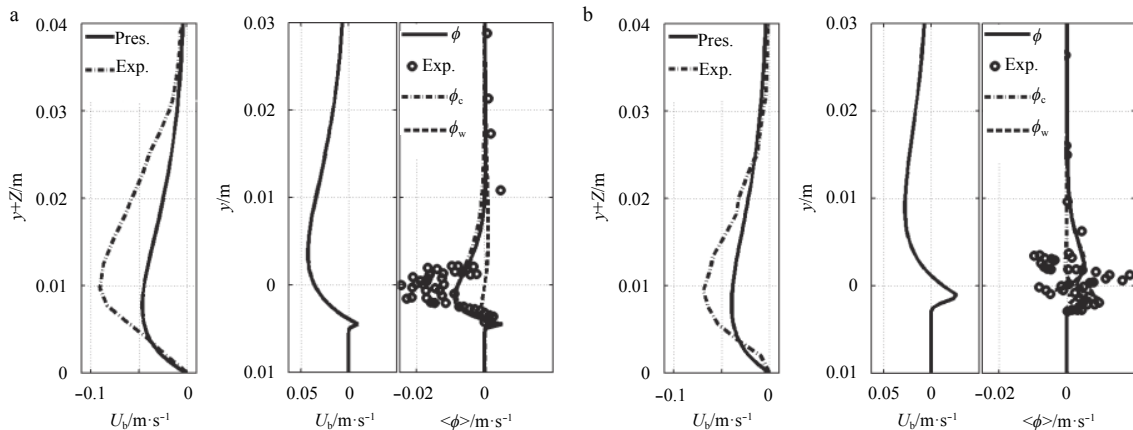


Fig. 5. Net current and sediment flux generated by velocity skewness ($T=7.5$ s, $U_t=0.9$ m/s and $U_{max}=U_c=1.5$ m/s). a. $D=0.13$ mm and b. $D=0.46$ mm.

present prediction agrees reasonably with the experiment and Chen et al. (2018c).

For $D=0.13$ mm (Fig. 5a), offshore ϕ_c almost expands to the whole sheet flow layer accordingly, and closely coincides with net ϕ , which means the offshore net ϕ is mainly caused by net U_b , instead of previous only phase-lag. Large phase-residual only makes periodic Z and C almost constant, whereas the direction of net U_b caused by the asymmetric development of δ_b decides the net ϕ direction. While for $D=0.46$ mm, the phase-residual is much small, the Z near flow crest is much larger than that during T_r . In Fig. 5b, ϕ_c is onshore and relatively large near bottom of the sheet flow layer, and is offshore and relatively small almost above the initial bed corresponding to net U_b , because the C decreases along y . Generally, averaged net ϕ is dominated by ϕ_c in the bottom of sheet flow layer for $D=0.46$ mm due to the mobile bed effect. Offshore net U_b above the initial bed is not important for net ϕ in $D=0.46$ mm case, because it cannot expand to the bottom with high C .

Figure 6 shows the instantaneous q , with formulas including: (1) Ribberink (1998) without acceleration; (2) Nielsen (2006) and Gonzalez-Rodriguez and Madsen (2007) considering acceleration. The q magnitude decreases with the increment of D (Figs 6a and b) due to the decrement of Z . The phase-residual of $D=0.13$ mm is very large that Z and q near the flow trough ($t/T=0.6-0.8$) are close to flow crest ($t/T=0.15-0.25$), which is important to offshore net q . In addition, the asymmetric δ_b leads to a relatively large U_b in the offshore flow (Eq. (3)) and offshore net U_b (Fig. 5a). This process is clearly illustrated in Fig. 6c with a comparison of $\text{sgn}(U)|U/U_{\max}|^n$. $q/q_{\max}=U/U_{\max}$ can be used with very large phase-residual for a symmetric δ_b (Chen et al., 2018b). In addition, the offshore U_b in $D=0.13$ mm is relatively enlarged because of relatively small δ_b (Eq. (3)), which results in $q/q_{\max}<U/U_{\max}$ near the flow trough ($t/T=0.6-0.8$) (Fig. 6c). Thus, the integration of q/q_{\max} is smaller than the integration of U/U_{\max} , which is offshore and in agreement with flux in Fig. 5a (Chen et al., 2018c).

In Fig. 6b, all formulas can be adequately used. The suspen-

ded sediment amount and the phase-lag are much small in this case, thereby leading to small amplitude of q , and a much stronger onshore Z and q than those at offshore due to velocity skewness. With small phase-lag, the relation $Z/D \propto \theta$ can almost be used (Fig. 3b), and $q/q_{\max}=(U/U_{\max})^3$, which is close to the instantaneous formulas without phase-residual, can be used for approximation (Fig. 6d), corresponding to an onshore integration of q/q_{\max} , i.e., $(U/U_{\max})^3$ (Chen et al., 2018c). The velocity skewness makes a much stronger q at flow crest than that at flow trough and generates onshore net rate, in agreement with Fig. 5b that the offshore U_b caused by the asymmetric development of δ_b is not important due to the small phase-lag. The effect of the velocity skewness is contributed by the phase-lag and asymmetric δ_b . In turn, only present prediction agrees with experiment well, especially the tendency with D (Figs 6a and b) and obviously offshore q (Fig. 6a) caused by large phase-residual and asymmetric δ_b .

3.2 Purely acceleration-skewed flows

In the purely acceleration-skewed flows, the Z is first shown in Fig. 7 for the same $T=6$ s and $U_{\max}=U_c=U_t=1.3$ m/s, where the phase-shift and the phase-residual are similar to Chen et al. (2018b). Ψ is 0.62 for $D=0.15$ mm case and is 0.08 for $D=0.46$ mm case. Correspondingly, the phase-shift for $D=0.15$ mm in Fig. 7a is about $0.07t/T$, which is larger than $0.02t/T$ for $D=0.46$ mm in Fig. 7b. Owing to the phase-residual, the classical relation $Z/Z_{\max}=\theta/\theta_{\max}$ cannot be used in Fig. 7a. The minimum Z near flow reversal in Fig. 7a is also larger than that in Fig. 7b. The periodic variation of Z is small in Fig. 7a due to large phase-residual, whereas the variation in Fig. 7b is much obvious. In Fig. 7, Z near flow crest ($t/T=0.18$) is larger and more sediment is carried up than that near flow trough ($t/T=0.82$), because the shear stress at flow crest is larger than that at flow trough (Suntoyo et al., 2008).

Notice the boundary layer has short time ($T_{a,c}$) for U to reach U_c due to the acceleration skewness (Nielsen, 1992), but has much time ($T_{a,t}$) for U to reach $-U_t$. δ_b is proportional to the oscillatory flow orbital amplitude and related to acceleration time.

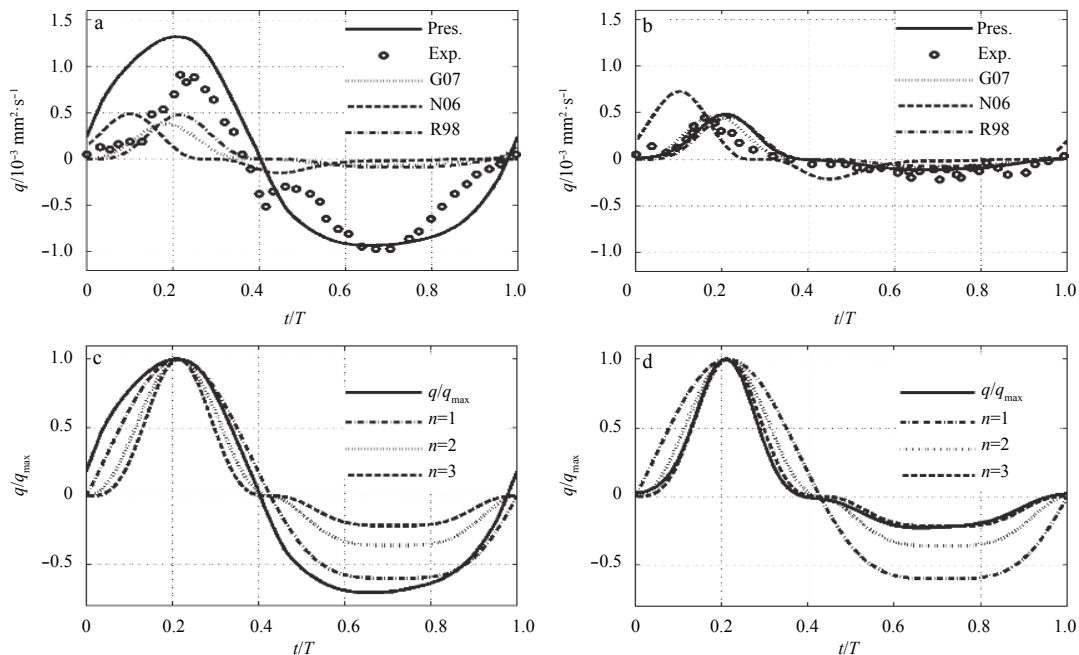


Fig. 6. Instantaneous q in purely velocity-skewed flow ($T=7.5$ s, $U_t=0.9$ m/s and $U_{\max}=U_c=1.5$ m/s). a. $D=0.13$ mm, b. $D=0.46$ mm, c. $D=0.13$ mm, and d. $D=0.46$ mm.

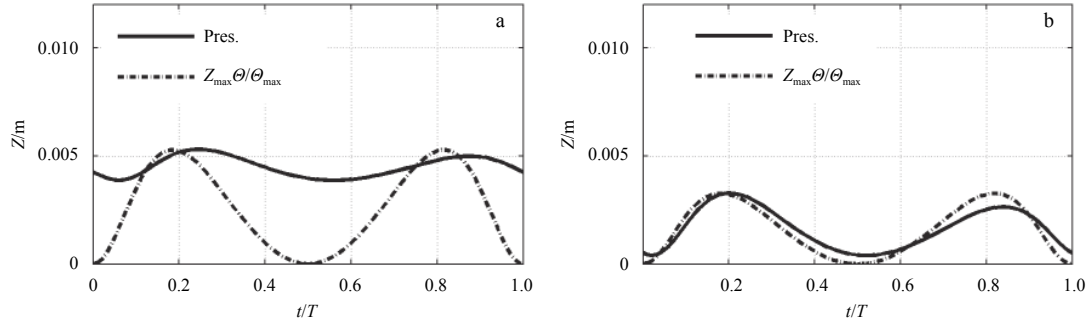


Fig. 7. Instantaneous Z in purely acceleration-skewed flow ($T=6$ s and $U_{\max}=U_c=U_t=1.3$ m/s). a. $D=0.15$ mm, $\beta=0.70$; and b. $D=0.46$ mm, $\beta=0.70$.

Figure 8 shows the corresponding δ_b used in Eq. (3), where the developments of onshore acceleration and offshore acceleration stages are different due to the acceleration skewness, and δ_b near the flow crest is smaller than that near the flow trough. δ_b decreases near flow crest and increases near flow trough with the increment in β , which results in a large U_b near flow crest and a relatively small U_b near flow trough in Eq. (3), thereby leading to onshore net U_b based on $y+Z$ and y (Fig. 9) in agreement with van der A et al. (2011) and Chen et al. (2018b). Onshore ϕ_c resulting from net U_b is also shown in Fig. 9, and can be illustrated by the mobile bed effect (Chen et al., 2018b) which is important for the onshore net sediment transport. The effect of acceleration is related to the development of the boundary layer (Chen et al.,

2018b). The net U_b magnitude is larger than Chen et al. (2018b) because the turbulence asymmetry (Ruessink et al., 2011) is not considered in Eq. (3). However, Eq. (4) is based on a constant sediment mixing efficient assumption near the bed, which leads to a smaller suspended sediment concentration than Chen et al. (2018b), and the net sediment transport rate validation in Fig. 2 is still good.

The wave related ϕ_w and total flux ϕ are also shown in Fig. 9. Averaged ϕ profiles in Figs 9a and b have the same shape, which is onshore at every location. The averaged ϕ decreases with the increment of D at every location for the same acceleration parameter β . Also, the averaged ϕ decreases with the decrement of β for the same D in agreement with the development of the bound-

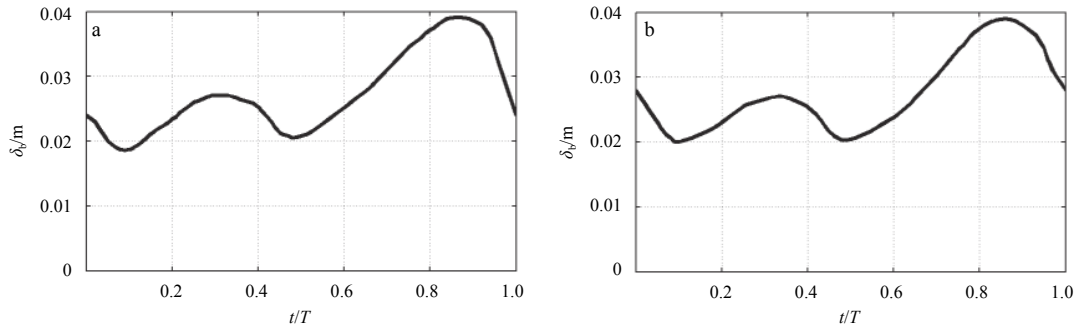


Fig. 8. Boundary layer thickness in purely acceleration-skewed flow ($T=6$ s and $U_{\max}=U_c=U_t=1.3$ m/s). a. $D=0.15$ mm, $\beta=0.70$; and b. $D=0.46$ mm, $\beta=0.70$.

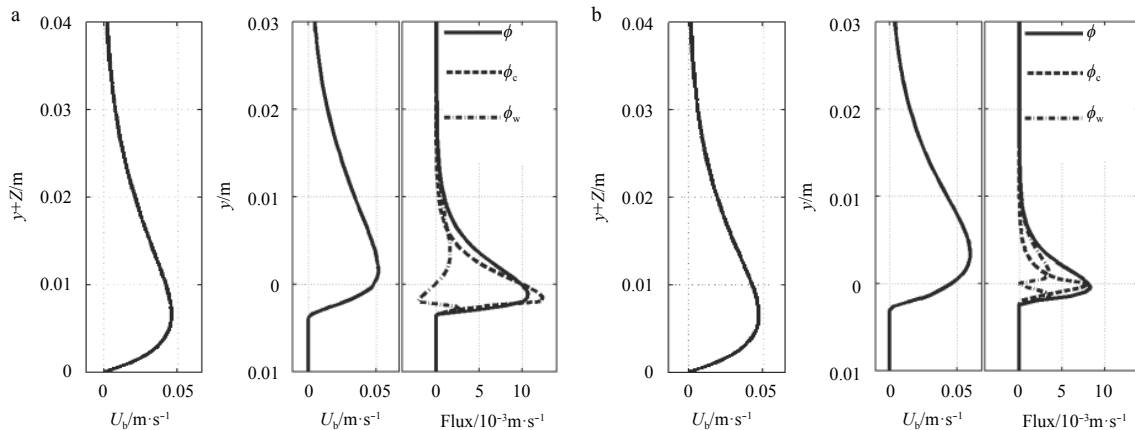


Fig. 9. Net current and flux generated by acceleration skewness ($\beta=0.70$, $T=6$ s and $U_{\max}=U_c=U_t=1.3$ m/s). a. $D=0.15$ mm and b. $D=0.46$ mm.

ary layer related to the acceleration skewness, where the boundary layer difference between the onshore acceleration and the offshore acceleration stages are decreased by the decrement of β . Otherwise, the averaged ϕ is 0 without the acceleration skewness, and U reverts to sinusoidal flow. Onshore ϕ_c and ϕ expand to the whole sheet flow layer (Fig. 9) corresponding to the net U_b (Chen et al., 2018b). The conclusion is confirmed that onshore net U_b caused by the asymmetric development of δ_b plays a very important role in the total ϕ .

Following Figs 7–9, the present computed instantaneous q/q_{\max} is shown in Fig. 10. The q/q_{\max} in the onshore flow stage can be approximated by $\text{sgn}(U)|U/U_{\max}|^n$ (Chen et al., 2018b). The q is not 0 at flow reversal due to the phase-lead. The same as Chen et al. (2018b), q_c is always larger than q_v , corresponding to the onshore net q . This is important for the estimation of onshore net q , which increases with decreasing D and increasing β (van der A et al., 2010). The less time developed δ_b at the flow crest is smaller than that at the flow trough ($T_{a,c} < T_{a,v}$) (Fig. 8).

With the increment in β , δ_b decreases near the flow crest and increases near the flow trough, thereby enlarges the δ_b difference between the onshore acceleration and offshore acceleration stages. Thus, U_b near flow crest is larger than near the flow trough (Eq. (2)), and Z and q near the flow crest are larger with more sediment carried up than those near the flow trough (Fig. 7). The difference of δ_b , U_b and Z between the onshore acceleration and offshore acceleration stages are key factors for the onshore net q generated in the purely acceleration-skewed flow. The effect of acceleration skewness is confirmed mainly the results of the asymmetric development of the boundary layer between the onshore acceleration and offshore acceleration stages. Furthermore, $n \geq 3$ can be applied in Figs 10b and d. This is in agreement with (Chen et al., 2018b) when Z can be approximated by U^2 in Fig. 7b, and coincides with bedload formulas without phase-lag, which implies that onshore net q still exists without phase-lag due to acceleration skewness.

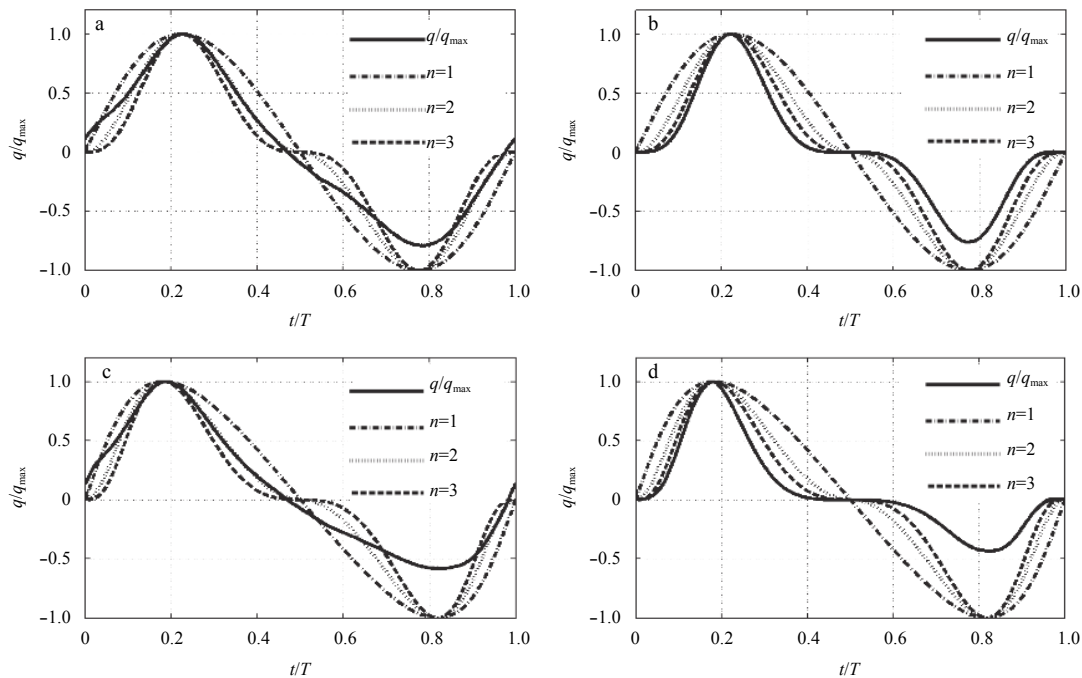


Fig. 10. Instantaneous sediment transport rate in purely acceleration-skewed flow ($T=6$ s and $U_{\max}=U_c=U_t=1.3$ m/s). a. $D=0.15$ mm, $\beta=0.58$; b. $D=0.46$ mm, $\beta=0.58$; c. $D=0.15$ mm, $\beta=0.70$; and d. $D=0.46$ mm, $\beta=0.70$.

4 Conclusions

A qualitatively analytical model is utilized to study the sediment transport under skewed asymmetric oscillatory sheet flow conditions with the essential phase-lead, the boundary layer thickness and the erosion depth given by a two-phase model which contains the rheological characteristic of sediment, and the enduring-contact, inertial, and fluid viscosity effects in the sediment pressure and stress. The mass conservation, the skewed asymmetric free stream velocity, and the exponential approaches of the boundary layer velocity and the sediment concentration are contained in the analytical model.

The increment of exponents in the power function between the sediment transport rate and velocity is confirmed by the decrement of phase-lag effect. Net boundary layer current and flux are obtained, and the contributions of phase-lag and boundary layer development to sediment flux and sediment transport

rate for skewed asymmetric oscillatory sheet flow are clearly shown. In conclusion for sediment transport in the purely velocity-skewed oscillatory sheet flow, the effect of the velocity skewness is the main cause of the phase-lag and asymmetry of the boundary layer between onshore and offshore stages. In conclusion for sediment transport in the purely acceleration-skewed oscillatory sheet flow, the effect of the acceleration skewness is the main cause of the asymmetry of the boundary layer between the onshore acceleration and offshore acceleration stages.

References

- Abreu T, Silva P A, Sancho F, et al. 2010. Analytical approximate wave form for asymmetric waves. *Coastal Engineering*, 57(7): 656–667
- Chen Xin, Li Yong, Chen Genfa, et al. 2018c. Generation of net sediment transport by velocity skewness in oscillatory sheet flow. *Advances in Water Resources*, 111: 395–405

- Chen Xin, Niu Xiaojing, Yu Xiping. 2013. Near-bed sediment condition in oscillatory sheet flows. *Journal of Waterway, Port, Coastal, and Ocean Engineering*, 139(5): 393–403
- Chen Xin, Wang Fujun, Tang Xuelin, et al. 2018a. Sediment flux based model of instantaneous sediment transport due to pure velocity-skewed oscillatory sheet flow with boundary layer stream. *Coastal Engineering*, 138: 210–219
- Chen Xin, Wang Fujun, Tang Xuelin. 2018b. Analytical approach of sheet flow transport in purely acceleration-skewed oscillatory flow. *International Journal of Sediment Research*, 33(3): 234–242 doi: [10.1016/j.ijsrc.2018.05.001](https://doi.org/10.1016/j.ijsrc.2018.05.001)
- Dibajnia M. 1991. Study on nonlinear effects in beach processes [dissertation]. Tokyo, Japan: University of Tokyo
- Dohmen-Janssen C M. 1999. Grain size influence on sediment transport in oscillatory sheet flow [dissertation]. Delft, the Netherlands: Delft University of Technology
- Dong Le Phuong, Sato S, Liu Haijiang. 2013. A sheetflow sediment transport model for skewed-asymmetric waves combined with strong opposite currents. *Coastal Engineering*, 71: 87–101
- Gonzalez-Rodriguez D, Madsen O S. 2007. Seabed shear stress and bedload transport due to asymmetric and skewed waves. *Coastal Engineering*, 54(12): 914–929
- Hassan W N M, Ribberink J S. 2010. Modelling of sand transport under wave-generated sheet flows with a RANS diffusion model. *Coastal Engineering*, 57(1): 19–29
- Lee C H, Low Y M, Chiew Y M. 2016. Multi-dimensional rheology-based two-phase model for sediment transport and applications to sheet flow and pipeline scour. *Physics of Fluids*, 28(5): 053305
- Li Ming, Pan Shunqi, O'Connor B A. 2008. A two-phase numerical model for sediment transport prediction under oscillatory sheet flows. *Coastal Engineering*, 55(12): 1159–1173
- Nielsen P. 1992. Coastal bottom boundary layers and sediment transport. In: *Advanced Series on Ocean Engineering*. vol 4. Singapore: World Scientific Publication
- Nielsen P. 2006. Sheet flow sediment transport under waves with acceleration skewness and boundary layer streaming. *Coastal Engineering*, 53(9): 749–758
- Nielsen P, Guard P A. 2010. Vertical scales and shear stresses in wave boundary layers over movable beds. In: *Proceedings of 32nd International Conference on Coastal Engineering*. Shanghai, China: ICCE, doi: [10.9753/icce.v32.sediment.1](https://doi.org/10.9753/icce.v32.sediment.1)
- O'Donoghue T, Wright S. 2004a. Concentrations in oscillatory sheet flow for well sorted and graded sands. *Coastal Engineering*, 50(3): 117–138
- O'Donoghue T, Wright S. 2004b. Flow tunnel measurements of velocities and sand flux in oscillatory sheet flow for well-sorted and graded sands. *Coastal Engineering*, 51(11–12): 1163–1184
- Ribberink J S. 1998. Bed-load transport for steady flows and unsteady oscillatory flows. *Coastal Engineering*, 34(1–2): 59–82
- Ribberink J S, Al-Salem A A. 1995. Sheet flow and suspension of sand in oscillatory boundary layers. *Coastal Engineering*, 25(3–4): 205–225
- Ruessink B G, Michallet H, Abreu T, et al. 2011. Observations of velocities, sand concentrations, and fluxes under velocity-asymmetric oscillatory flows. *Journal of Geophysical Research*, 116(C3): C03004, doi: [10.1029/2010JC006443](https://doi.org/10.1029/2010JC006443)
- Ruessink B G, van den Berg T J, van Rijn L C. 2009. Modeling sediment transport beneath skewed asymmetric waves above a plane bed. *Journal of Geophysical Research*, 114(C11): C11021, doi: [10.1029/2009JC005416](https://doi.org/10.1029/2009JC005416)
- Suntoyo, Tanaka H, Sana A. 2008. Characteristics of turbulent boundary layers over a rough bed under saw-tooth waves and its application to sediment transport. *Coastal Engineering*, 55(12): 1102–1112
- van der A D A, O'Donoghue T, Davies A G, et al. 2011. Experimental study of the turbulent boundary layer in acceleration-skewed oscillatory flow. *Journal of Fluid Mechanics*, 684: 251–283
- van der A D A, O'Donoghue T, Ribberink J S. 2010. Measurements of sheet flow transport in acceleration-skewed oscillatory flow and comparison with practical formulations. *Coastal Engineering*, 57(3): 331–342
- Watanabe A, Sato S. 2004. A sheet-flow transport rate formula for asymmetric, forward-leaning waves and currents. In: *Proceedings of 29th International Conference on Coastal Engineering*. Lisbon, Portugal: ICCE, 1703–1714
- Yuan Jing, Madsen O S. 2015. Experimental and theoretical study of wave-current turbulent boundary layers. *Journal of Fluid Mechanics*, 765: 480–523